第 33 卷第 9 期
2017 年 9 月

无 机 化 学 学 报
CHINESE JOURNAL OF INORGANIC CHEMISTRY

Vol.33 No.9
1618-1624

微/纳复合型可见光光电材料 Ag-石墨烯-TiO_2 的制备及应用

王翠娥* 王 宁 刘新华
(安徽工程大学纺织服装学院,芜湖 241000)

摘要: 基于静电纺丝技术构筑了稳定均一的 Ag-石墨烯-TiO_2 纳米复合纤维; 并利用 SEM、TEM、XRD、EDS 和 Raman 等表征了材料的微观结构与组分;随后,我们研究了该复合纤维在可见光下的光电转换性能。结果表明:掺杂既可降低 TiO_2 材料的禁带宽度,也能减缓光生电子与空穴的复合淬灭;Ag 纳米晶的局域等离激元可增强纤维对可见光的吸收,石墨烯能促进光生电子与空穴的有效分离;可见光条件下,相比较于单一的 TiO_2 纳米纤维,复合纤维的光电流密度提高 4 倍,达到 0.81 $\mu A \cdot cm^{-2}$。

关键词: 静电纺丝; TiO_2; Ag; 石墨烯; 光电转换
中图分类号: O611.3 **文献标识码**: A **文章编号**: 1001-4861(2017)09-1618-07
DOI:10.11862/CJIC.2017.186

Electrospun Fibrous Ag-Graphene-TiO_2 with Enhanced Photocurrent Response under Visible-Light Illumination

WANG Cui-E* WANG Ning LIU Xin-Hua
(*College of Textiloues and Clothing, Anhui Polytechnic University, Wuhu, Anhui* 241000, *China*)

Abstract: A highly-uniform nanofiber of Ag-graphene-TiO_2 was successfully fabricated by the electrospinning technique, which exhibited significantly increased visible light absorption (λ > 420 nm) and improved photocurrent response. The Ag nanoparticles (AgNPs) and graphenes located in TiO_2 fibers induced an increase in the visible-light photocurrent response. The photocurrent density of Ag-graphene-TiO_2 fibers is 4-fold higher than the pristine TiO_2 fibers under visible light. The increased photocurrent response in visible light region is resulted from the strong interaction between TiO_2 fibers and graphene sheets, as well as the localized surface plasmon resonance of AgNPs.

Keyword: electrospinning; TiO_2; Ag; graphene; photocurrent

0 Introduction

TiO_2 has been attracted much attention for their potential application in the field of dye-sensitized solar cells[1], photocatalysts[2], electrocatalysts[3], self-cleaning materials[4], antibacterial coatings[5], and gas sensors[6]. Compared with conventional TiO_2 particles, TiO_2 fibers have greater surface-to-volume ratio[7], and their porous structure allow for higher surface active sites for effective catalysis. However, the photo activity efficiency of TiO_2 fiber using natural sunlight is currently very limited due to wide band gap energy (3.2 eV for anatase)[8], as well as the low quantum yield caused by fast recombination of photo-generated electron-hole pairs. Therefore, to inhibit the recombination of photo-generated electron-hole pairs and to

收稿日期:2017-03-01。收修改稿日期:2017-07-03。
国家自然科学基金(No.21302001)、安徽省高校优秀青年人才支持计划重点项目(No.gxyqZD2016119)和安徽工程大学中青年拔尖人才项目(No.2016BJRC013)资助。
*通信联系人。E-mail:wangcuie@ahpu.edu.cn

make TiO_2 responsive to visible light region are two critical ways to improve the photocurrent density of TiO_2 under solar irradiation.

Recently, much effort was made by doping with metal or nonmetal elements, such as Au[9], Ag[10], Fe[11], N[12], S[13], I[14], as well as sensitization with organic dyes[15], conducting polymer[16] and semiconductor[17]. Among these attempts, noble metallic nanoparticles have been intensively studied because they can efficiently promote the photo response primarily by extending the optical absorption to the visible light region and increasing the number of photoexcited electrons due to the enhanced near-field amplitude. In these noble metallic nanoparticles, silver nanoparticle is a popular choice, which can result in strong and broad absorption band in the visible light region[18]. Meanwhile, another approach to optimize the photocurrent of TiO_2 is to retard surface and bulk recombination of photogenerated electron-hole pairs in TiO_2 during a photocatalytic process. A narrow band gap semiconductor, electron donors/acceptors and hole scavengers have been proven to be available way for inhibiting electron-hole pair recombination[19]. Graphene is a good candidate for scavenging of photogenerated electrons mainly because of its superior charge transport properties, large specific surface area and two-dimensional planar conjugation structure[20].

Motivated by the above concerns, in this work, we describe an efficient way to synthesis of Ag-graphene-TiO_2 fiber with high photocurrent density by electrospinning method. The adopted electrospinning approach ensures not only the successful incorporation of AgNPs and graphenes into TiO_2 fibers substrate but also the high dispersion of AgNPs and graphenes into TiO_2 fibers without aggregation. By simply tuning the precursor concentration or reaction temperature, we can optimize the AgNP or graphene density in fibers. Moreover, the fibrous Ag-graphene-TiO_2 allows light to pass through to illuminate.

As illustrated in Scheme 1, under simulated solar light irradiation, the electrons in the valence band (VB) of TiO_2 are excited to the corresponding conduction band (CB). Then the electrons in the CB of TiO_2 migrate into the metal Ag (electron transfer: TiO_2 to Ag) through the Schottky barrier because the CB of the TiO_2 is higher than that of the loaded metal Ag. This process of electron transfer is faster than the electron-hole recombination between the VB and CB of the TiO_2. Thus, the electrons in the CB of TiO_2 can be stored in the Ag component. Furthermore, tightly bound graphene to TiO_2 accelerates electron transfer from the excited MB to TiO_2 via graphene nanosheets, retard the combination of photogenerated electron-hole pairs and thus accelerating visible-light-driven photocurrent.

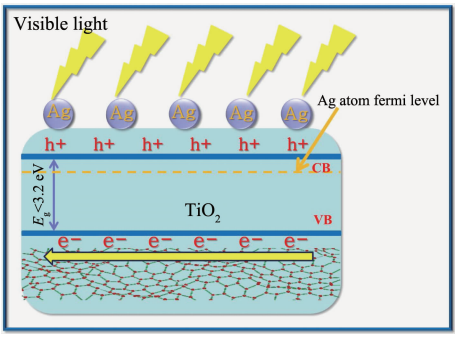

Scheme 1　Typical photoresponses of Ag-graphene-TiO_2 fiber under visible light irradiation

1　Experimental

1.1　Synthesis of Ag-graphene-TiO_2 fibers

In a typical procedure, 0.6 mL tetrabutyltitanate (TBT) and 4 g polyvinylpyrrolidone (PVP) were dissolved into a mixture solution of 6 mL ethanol and 0.6 mL acetic acid. After the mixture was stirring for 1 h, 30 mg silver nitrate and different amount of graphene powder were mixed together. The solutions were then homogeneously ultrasonicated for 60 min, and the reducing agent (containing 0.2 mol·L^{-1} $NaBH_4$) was added dropwise to the above solution still with continuous stirring. The electrospinning was carried out at 16 kV through a DW-P503-1AC high-voltage supplier, and the feed rate was set at 0.4 mL·h^{-1} by using a JZB-1800D microinfusion pump. The nanofibers were collected on electrically grounded aluminum foil, and the distance between the aluminum foil and the tip of needle was 15 cm. Finally, the as-spun nanofibers were then calcined at 500 ℃ for 2 h in air before cooling to room temperature. Pure TiO_2

nanofibers were similarly prepared but without the addition of graphene and $AgNO_3$ solution and the reducing agent, and the Ag-TiO_2 fibers were prepared without graphene.

1.2 Preparation of photoelectrodes

In the experiment, glass carbon electrodes (GCEs) with 3 mm diameter were carefully polished to obtain a mirror-like surface. Then, the Ag-graphene-TiO_2 fibers dispersion was dripped onto the GCE.

1.3 Photoelectrochemical measurements

The photoelectrochemical performances of the Ag-TiO_2, pristine TiO_2, and Ag-graphene-TiO_2 fibers under visible light irradiation were recorded on an electrochemical workstation (Model CHI660A, CH Instruments Co.). The photoelectron chemical cell was a three-electrode system: an Ag-TiO_2, pristine TiO_2, or Ag-graphene-TiO_2 photoelectrode located in the middle of the cell as a working electrode, Ag/AgCl electrode as reference, and a platinum wire electrode as a counter electrode. The photoelectrode was exposed to visible light to measure closed-circuit photocurrent. The light source was a 160-W high-pressure mercury lamp with a UV cutoff filter (>420 nm). All measurements were carried out at room temperature. The electrolyte was 0.5 mol·L^{-1} Na_2SO_4 aqueous solution. The working electrode was activated in the electrolyte for 2 h before measurement. The samples were irradiated with lamp located 10 cm away and typically irradiated at intervals of 25 s. Experiments were obtained at different fixed applied potentials, from −0.3 V to +0.5 V.

2 Result and discussion

2.1 Structure and morphology of Ag-graphene-TiO_2 nanocomposite

The formation of Ag-graphene-TiO_2 nanocomposite was confirmed by scanning electron microscopy (SEM) analysis, and its representative images are presented in Fig.1. Fig.1(a) and 1(c) show a representative SEM image of low and high magnifications of $AgNO_3$-graphene-Ti (Ⅳ) isopropoxide/PVP composite fibers. The as-made $AgNO_3$-graphene-Ti(Ⅳ)isopropoxide /PVP composite fibers have a smooth surface; the diameters of these fibers are 300~500 nm. Fig.1 (b) and 1(d) show SEM image of low and high magnifications of Ag-gaphene-TiO_2 composite fibers, the calcined process would cause some changes of the smooth cylindrical shape of the bers both in general shape and superficial roughness, the diameters of the TiO_2 nanofibers are 100~250 nm, and the length of the fibers reached a few millimeters length.

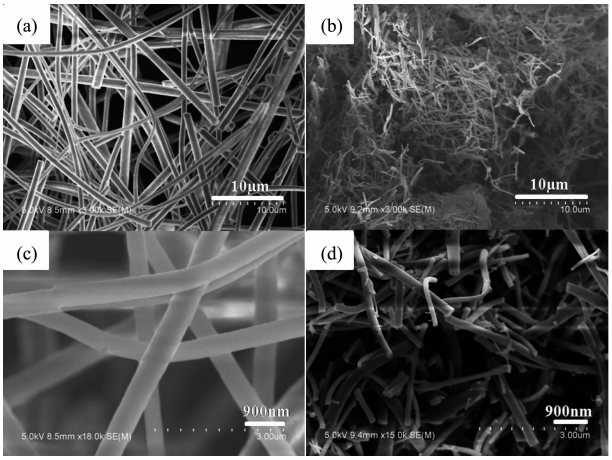

Fig.1 (a) and (c) SEM images of $AgNO_3$,graphene-Ti(Ⅳ) isopropoxide/PVP composite nanofiber surface; (b) and (d) SEM images Ag-gaphene-TiO_2 nanofiber suface calcined at 500 ℃

Fig.2 shows typical TEM images of the products. After calcined, nanofiber with diameters of 200 nm is observed. It indicates that the formation of Ag-gaphene-TiO_2 nanofiber.

TG-DSC data for precursors $AgNO_3$-graphene-Ti (Ⅳ) isopropoxide/PVP composite fibers, in air atmosphere, reveals that the substances show different thermal behaviors. This fact can be explained by the presence of graphene in the nanofiber. Another aspect observed was that the stoichiometry for decomposition,

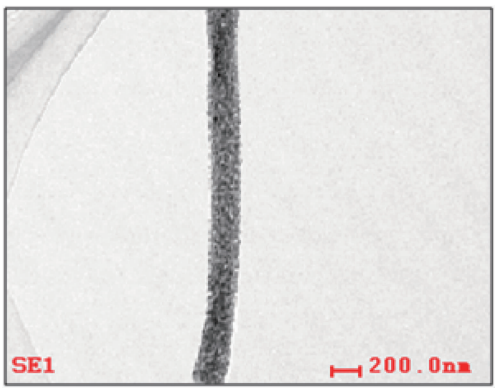

Fig.2 TEM image of Ag-gaphene-TiO_2 nanofiber

at 175 ℃, where the mass losses 36.4% in the first decline stages, corresponding to a transformation of the tetrabutyltitanate molecules to $Ti(OH)_4$, at 330 ℃, mass losses 28.3% in the second decline stages, due to decomposition and carbonization of polyvinylpyrrolidone, finally, an aspect which was observed by the tangent TG analysis, between 450 and 500 ℃, was that the carbon oxygenolysis, with 20.1% of mass loss, this mass loss would correspond to carbon oxygenolysis, the carbon is mainly derived from the carbonization of polyvinylpyrrolidone, and graphene on surface of the fiber.

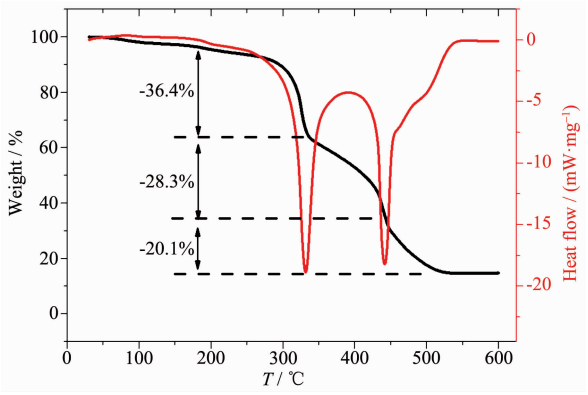

Fig.3　TG-DSC curve of precursors $AgNO_3$-graphene-Ti(Ⅳ) isopropoxide/PVP composite fibers

The obtained samples were further characterized by EDS mapping characterization. The EDS mapping images (Fig.4) indicate that the sample contains Ti, O, Ag and C elements, suggesting the co-existence of titanium dioxide, Ag nanoparticles and gaphene. It is clearly shown that Ag (Fig.4c) and C elements (Fig. 4d) are well dispersed in the samples, suggesting that the Ag nanoparticles and gaphene were uniformly distributed throughout the fiber. Hence one can see that at 500 ℃, the graphene embedded in the TiO_2 fiber was not oxidized and decomposed, and was successfully retained in the fiber carrier.

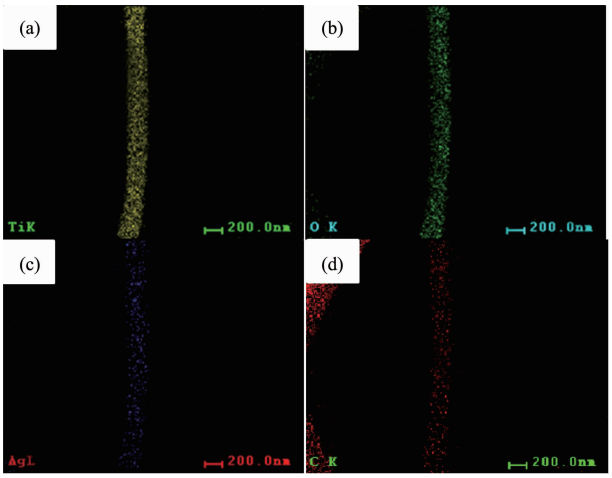

Fig.4　TEM (EDS) mapping image of Ti element (a), O element (b), Ag element (c) and C element (d)

Fig.5(a) shows the XRD patterns of the TiO_2 and Ag/TiO_2/graphene fibers sample. The structure of TiO_2 was compared with the Joint Committee for Powder Diffraction Standards (JCPDS) data (File Card No.21-1272) and was found to be in anatase and rutile form, and metallic silver phases (JCPDS File Card No.89-3722) were detected in their patterns. However, the reflection peak of graphene is absent because of its low content. EDX measurement results further confirmed the existence of graphene in the composite. As shown in Fig.5(b), peaks of carbon, appearing clearly at about 0.2 keV is attributable to graphene. Besides,

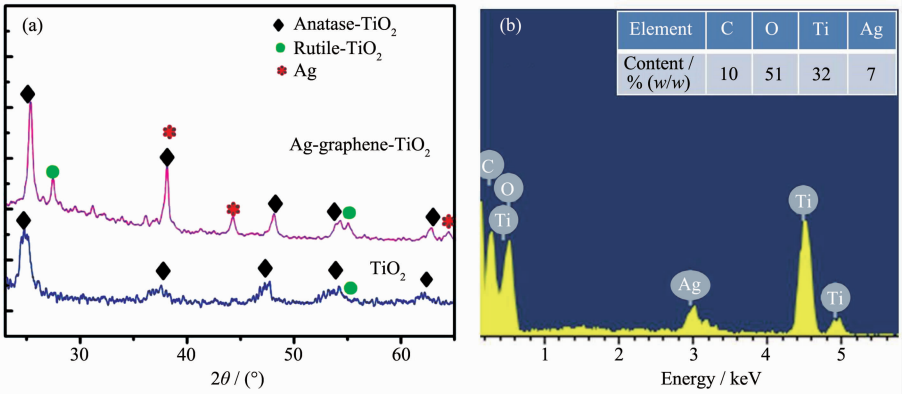

Fig.5　XRD pattern of the TiO_2 fibers and Ag-graphene-TiO_2 fibers (a) and EDX spectrum (b) of the as-prepared Ag-graphene-TiO_2 fibers

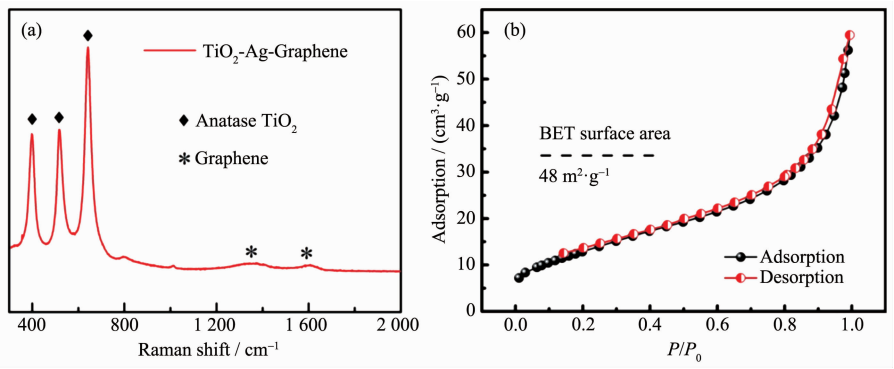

Fig.6 Raman spectrum (a) and Nitrogen adsorption-desorption isotherm (b) of the as-prepared Ag-gaphene-TiO_2 nanofibers, respectively

three peaks are clearly located around 0.4, 4.5 and 5 keV, these are related to the characteristics of titanium, while the strong spectrum at about 3 and 0.5 keV originates from the silver and oxygen. Energy dispersive X-ray spectroscopy (EDX) mapping analysis shows that the composite fiber is composed of Ti, O, C, and Ag with uniform distribution (Fig.4). The mass percent of component Ag and C estimated from EDX spectrum were about 7% and 10%, respectively (Fig.5b).

Fig.6(a) shows the Raman spectra of Ag-grapene-TiO_2 nanofibers. Two prominent peaks corresponding to the G and D bands of graphene appeared at 1 347 and 1 598 cm^{-1}, respectively. In particular, the bands at 398, 456, and 673 cm^{-1} are presented implying the existence of the anatase TiO_2, Ag NPs are not detected in Raman spectra, due to low content. The nitrogen adsorption-desorption isotherms of the as-obtained Ag-gaphene-TiO_2 shown in Fig.6(b). The Brunauer-Emmett-Teller (BET) specific surface area of the nanofibers was 48 $m^2 \cdot g^{-1}$, very similar to TiO_2 nanofibers and P-25 TiO_2 nanoparticles[21].

2.2 Photocurrent conversion properties of the electrodes decorated with Ag-gaphene-TiO_2 nanofibers

Fig.7a depicts the typical photocurrent versus time (*I-t*) response curves for TiO_2, Ag-TiO_2 and Ag-graphene-TiO_2 samples under visible-light irradiation. All the samples presented a rise and fall mode, changes in the photocurrent closely matched illumination over time. As shown in Fig.5a, the photocurrent density of the pristine TiO_2 nanofiber was 0.18 $\mu A \cdot cm^{-2}$, while

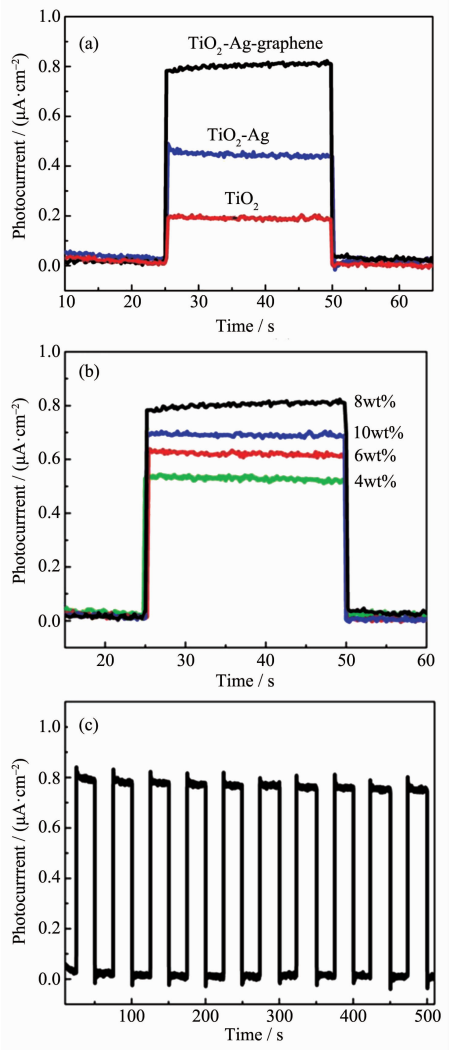

Fig.7 (a) Photocurrent transient responses at a constant potential of 0.5 V for different samples, (b) Recycle stability of Ag-graphene-TiO_2 under visible-light irradiation, (c) Photocurrent transient responses for different loaded graphene content in Ag-graphene-TiO_2 nanofiber

Ag-TiO_2 was 0.42 $\mu A \cdot cm^{-2}$, which is 2.3 times higher than those of the TiO_2. This result may be because of localized surface plasmon resonance of Ag nanoparticles on the TiO_2 nanofiber surface, which enhance its optical response to visible light region, thereby improving the photocurrent property. As expected, after introducing graphene, the photocurrent density increased remarkably, 4.5 and 1.93 times as much as that of TiO_2 and Ag-TiO_2, respectively. Ag-graphene-TiO_2 exhibited much higher photocurrent property, ascribe to the localized surface plasmon resonance (LSPR) of Ag NPs, high electron transfer and broad absorption in the visible light of graphene induce an activity promotion under visible light. The proportion of graphene is critical for the photocurrent activity, as shown in Fig.7(b), with increased graphene content from 4% to 8%(*w*/*w*), the photocurrent density of Ag-graphene-TiO_2 increased from 0.45 $\mu A \cdot cm^{-2}$ to 0.81 $\mu A \cdot cm^{-2}$, which is higher than those reported for the ZnO nanoparticle-decorated reduced graphene oxide composites[22], CuS/reduced graphene oxide nanocomposites[23], graphene oxide[24]. However, further increased graphene content from 8% to 10%(*w*/*w*), the photocurrent density of Ag-graphene-TiO_2 decreased to 0.7 $\mu A \cdot cm^{-2}$, This may be due to that high graphene load prevented TiO_2 from absorbing visible light, which in a rapid decreas e of irradiation. Therefore, the optimum doping content for graphene was 8%(*w*/*w*), which may be due to the balance between the increase in highest electron transfer and the decrease in light adsorption. Another important feature of Ag-graphene-TiO_2 is the reusability; photocurrent density was measured and repeated ten on-off cycles to examine the reusability. As shown in Fig.7(c), It was found the photocurrent density still maintained 95% after 10 on-off cycles, indicating high stability of Ag-graphene-TiO_2.

3 Conclusions

The present study demonstrates a novel method to prepare Ag-graphene-TiO_2 nanofibers with good dispersity. As a result, novel nanocomposites shows enhanced visible-light photocurrent activity as compared with those has been previously reported. The high photocurrent activity of the Ag-graphene-TiO_2 can be attributed to the synergistic effect originating from the enhanced optical response to visible light with Ag and fast electron transfer with graphene, resulting in increased photocurrent activity. The recycling test revealed that the Ag-graphene-TiO_2 prepared in this study was stable and effective for increasing the attainable photocurrent. Therefore, the approach described in this paper help improve the characteristics of photoelectric conversion systems. We estimate that this work provided a simple and effective strategy to fabricate composite photocurrent materials for applications.

References:

[1] Kim H S, Lee J W, Yantara N, et al. *Nano Lett.*, **2013**,**13**(6): 2412-2417

[2] (a)Wang D, Zhao L, Guo L H, et al. *Anal. Chem.*, **2014**,**86**(21): 10535-10539

(b)Izadyar S, Fatemi S. *Ind. Eng. Chem. Res.*, **2013**,**52**(32): 10961-10968

[3] (a)Yang Y, Wang H, Li J, et al. *Environ. Sci. Technol.*, **2012**, **46**(12):6815-6821

(b)Chang X, Thind S S, Chen A. *ACS Catal.*, **2014**,**4**(8):2616-2622

[4] Khajavi R, Berendjchi A. *ACS Appl. Mater. Interfaces*, **2014**, **6**(21):18795-18799

[5] Virkutyte J, Varma R S. *RSC Adv.*, **2012**,**2**(4):1533-1539

[6] Barreca D, Comini E, Ferrucci A P, et al. *Chem. Mater.*, **2007**, **19**(23):5642-5649

[7] Kim I D, Rothschild A, Lee B H, et al. *Nano Lett.*, **2006**,**6** (9):2009-2013

[8] Park J H, Kim S, Bard A J. *Nano Lett.*, **2006**,**6**(1):24-28

[9] Li J, Cushing S K, Zheng P, et al. *J. Am. Chem. Soc.*, **2014**, **136**(23):8438-8449

[10]Lu Q, Lu Z, Lu Y, et al. *Nano Lett.*, **2013**,**13**(11):5698-5702

[11]Su R, Bechstein R, Kibsgaard J, et al. *J. Mater. Chem.*, **2012**, **22**(45):23755-23758

[12]Lo H H, Gopal N O, Sheu S C, et al. *J. Phys. Chem. C*, **2014**, **118**(5):2877-2884

[13]Mamba G, Mamo M A, Mbianda X Y, et al. *Ind. Eng. Chem. Res.*, **2014**,**53**(37):14329-14338

[14]Etgar L, Gao P, Xue Z, et al. *J. Am. Chem. Soc.*, **2012**,**134** (42):17396-17399

[15]Roiati V, Giannuzzi R, Lerario G, et al. *J. Phys. Chem. C*, **2015**,**119**(13):6956-6965

[16]Ngaboyamahina E, Cachet H, Pailleret A, et al. *J. Electroanal. Chem.*, **2015**,**737**:37-45

[17]McEntee M, Stevanovic A, Tang W, et al. *J. Am. Chem. Soc.*, **2015**,**137**(5):1972-1982

[18](a)Lian Z, Wang W, Xiao S, et al. *Sci. Rep.*, **2015**,**5**:10461
(b)Choi Y, Kim H, et al. *ACS Catal.*, **2016**,**6**(2):821-828

[19]Linsebigler A L, Lu G, Yates J T. *Chem. Rev.*, **1995**,**95**(3):735-758

[20]Wang X, Fan L, Gong D, et al. *Adv. Funct. Mater.*, **2016**,**26**(7):1143-1143

[21]Mukherjee K, Teng T H, Jose R, et al. *Appl. Phys. Lett.*, **2009**,**95**(1):012101

[22]Tian J, Liu S, Li H, et al. *RSC Adv.*, **2012**,**2**:1318-1321

[23]Zhang Y, Tian J, Li H, et al. *Langmuir*, **2012**,**28**:12893-12900

[24]ZHANG Xiao-Yan(张晓艳), SUN Min-Xuan(孙明轩), SUN Yu-Jun(孙钰珺), et al. *Acta Phys.-Chim. Sin.*(物理化学学报), **2011**,**27**(12):2831-2835